

DESIGN-ORIENTED APPROACH FOR STRAIN-SOFTENING AND STRAIN-HARDENING FIBRE HYBRID REINFORCED CONCRETE ELEMENTS FAILING IN BENDING

M. Taheri¹, J.A.O. Barros², H. Salehian³

Abstract

In the present paper a design oriented model is proposed to evaluate the flexural resistance of elements of fibre reinforced concrete (FRC) of tensile strain-softening or tensile strain-hardening behaviour and strengthened longitudinally by steel bars in the tensile zone of a rectangular cross section. The cross sectional moment-curvature response predicted by this model is used in a numerical approach to predict the load-deflection relationship of beams failing in bending. To appraise the predictive performance of this approach, the results obtained in an experimental program with shallow beams of steel fibre reinforced self-compacting concrete and strengthened with distinct reinforcement ratios are compared to those estimated by the developed model. The predictive performance of the model is quite satisfactory, taking into account the simplified approaches adopted in order to have a closed form solution that can be used in the scope of design FRC elements failing in bending.

Keywords: Fibre reinforced concrete, Tensile strain-softening, Tensile strain-hardening, Longitudinal steel bars, Moment-curvature response; Flexural failure

1. Introduction

The benefits provided by the participation of discrete fibres in the reinforcement of cement-based structures are already well known by the scientific and technical community of the concrete technology. Discrete fibres can, in fact, decrease the crack opening and crack spacing of concrete elements, contributing to increase the load carrying capacity, the energy dissipation and the ductility at serviceability and at ultimate limit design states [1]. In consequence of the crack arrestment provided by the pullout resisting mechanisms offered by fibres bridging the crack surfaces, the durability and concrete integrity are also enhanced [2]. However, the potentialities of fibres as a reinforcement system are not yet well explored, mainly for structural applications, since models in a format adjusted for design practice, like closed-form solutions, are rare. Recently, Soranakom and Mobasher [3] developed a closed-form solution for the prediction of the moment-curvature

¹ Researcher, ISISE, Dep. Civil Eng., Minho University, Guimarães, Portugal, taheri@civil.uminho.pt

² Associate Prof., ISISE, Dep. Civil Eng., Minho University, Guimarães, Portugal, barros@civil.uminho.pt

³ PhD Student, ISISE, Dep. Civil Eng., Minho University, Guimarães, Portugal, salehian@civil.uminho.pt

relationship of rectangular cross section elements failing in bending, constituted by fibre reinforced concrete (FRC) that can have a tensile strain-softening (SS) or a tensile strain-hardening (SH) character [4]. A bilinear stress-strain softening diagram was utilized in [5] to study the FRC section strengthened with steel bars, composed by an abrupt stress decay branch (vertical branch) at crack initiation, followed by a constant residual tensile strength and a stress cut-off at a certain ultimate tensile strain. However, it is being recognized that between the crack initiation and the post-cracking residual strength phases, a transition softening branch should be adopted, since it has a significant contribution on the performance of FRC structural members, mainly at the serviceability limit states [6].

In the present work the model proposed in [3] is extended in order to derive a closed-form solution able of determining the moment-curvature relationship (MCR) of both SS or SH fibre reinforced concrete elements failing in bending that also includes tensile steel bars. Using the flexural stiffness (EI) provided by the MCR, a simple, but enough accurate numerical approach is developed that can predict the force-deflection relationship of statically determinate elements failing in bending. The predictive performance of the model was appraised by simulating experimental tests executed with steel fibre reinforced self-compacting concrete (SFRSCC) shallow beams reinforced with distinct steel reinforcing ratios.

2. Constitutive laws for the intervening materials

Tensile stress-strain relationship of FRC can be characterized in three different phases as depicted in Fig. 1a. The initial linear elastic behaviour is defined by an elastic tensile modulus (E) and concrete crack strain (ε_{cr}). For current practical applications of FRC, fibre reinforcement mechanisms have a negligible influence on this phase, therefore the E and ε_{cr} can be assumed equal to the corresponding values of the homologous plain concrete. Experimental evidence [7] shows that after crack initiation in SS-FRC, in general, an abrupt decay of the residual tensile strength occurred for a relatively low increase of tensile deformability, since this phase is mainly controlled by the fracture characteristics of the cement matrix. This second phase is, in a simplified way, assumed as a linear branch characterized by the post-cracking modulus E_{cr} and the transition strain ε_{trn} . These two variables are also used to simulate the second phase of SH-FRC, but in this type of high tensile and ductile FRC the ε_{trn} can be several times higher the ε_{cr} due to the formation of a diffuse crack pattern [8]. In the present approach, after the tensile transition phase, the tensile residual strength (σ_{cst}) is assumed constant up to the ultimate tensile strain (ε_{tu}), above which it is assumed that FRC loses its tensile capacity. Experimental research with SS-FRC shows that, in general, after a minimum post-crack residual strength, a pseudo-hardening phase occurred due to the fibre pullout mechanisms [7], followed by a smooth softening branch up to the complete loss of tensile load carrying capacity. Therefore, the amplitude of this third phase (between ε_{trn} and ε_{tu}) is, in general, of relatively high amplitude. In case of SH-FRC this third phase can be regarded the transition phase between the stabilization of the diffuse crack pattern and the formation of the failure crack (localization), which corresponds to an amplitude that, in general, is

smaller than the one corresponding to the second phase (between ε_{cr} and ε_{trn}). The third phase is, therefore, characterized by the residual tensile strength σ_{cst} .

The experimental research shows that for both SS- and SH-FRC the pre-peak compression behaviour is marginally affected by the presence of fibres, unless quite high content of fibres are used. In fact, the benefits of fibre reinforcement for the compression behaviour are most reflected in the compression softening phase, since a significant increase of the post-peak energy absorption capacity can be obtained, depending on the characteristics of the fibres and surrounding matrix [9]. Therefore, the simplified constitutive law represented in Fig. 1b is adopted to simulate the FRC in compression, which is the same one proposed in [3]. This law is composed by an initial linear branch characterized by the compressive Young's Modulus (E_c) up to the compressive "yield" strain (ε_{cy}), and continues with a constant value of compressive "yield" stress (σ_{cy}) up to the ultimate compressive strain (ε_{cu}), after which it is assumed that FRC loses the capacity of supporting compressive loads. In Fig. 1c is represented the idealized stress-strain relationship adopted for the steel bars, which is composed by an initial linear elastic branch, characterized by the elasticity modulus (E_s) up to the yield strain (ε_{sy}), and continues with a plastic response of a constant yield stress (σ_{sy}) up to attain the ultimate tensile strain (ε_{su}), after which it is assumed that the steel loses its tensile capacity. The symbols used for the characterization of the FRC are the same ones proposed in [3].

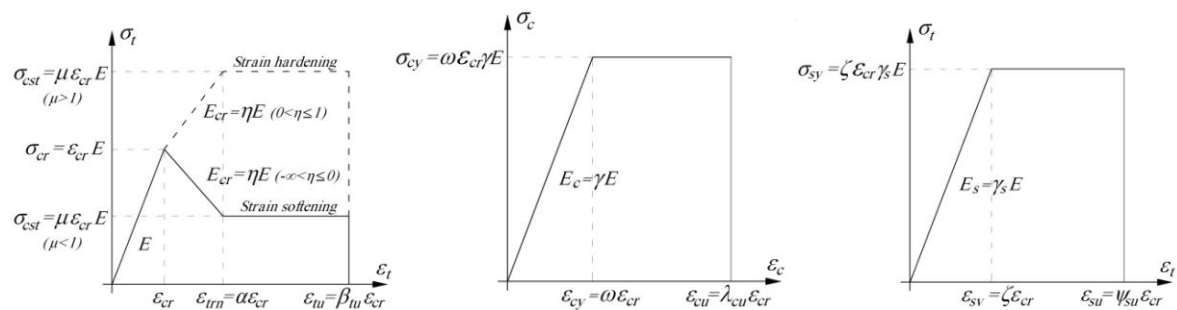


Fig. 1: Idealized stress-strain response of FRC: (a) tensile behaviour, (b) compression behaviour (based on [3]); and (c) idealized stress-strain diagram for steel bars.

3. Derivation of a closed-form solution for moment–curvature diagram

The closed-form solution is derived for a rectangular cross section of width and height of b and d , respectively, as shown in Fig 2. The reinforcement ratio of steel bars (ρ) is the quotient between the total area of steel bars (A_s) and the cross section area (bd). The concrete cover thickness of the steel bars is represented by d' . The tensile and the compressive stress variation of cross sectional components can be normalized by the FRC stress at crack initiation, σ_{cr} ($= E \varepsilon_{cr}$), in according to the following equations:

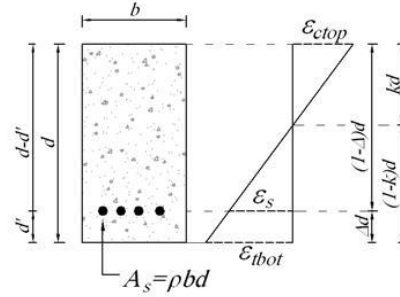


Fig. 2: Main variables that describe the geometry and the strain profile in a FRC reinforced rectangular cross section.

$$\frac{\sigma_t(\beta)}{E \varepsilon_{cr}} = \begin{cases} \beta & 0 < \beta \leq 1 \\ 1 + \eta(\beta - 1) & 1 < \beta \leq \alpha \\ \mu & \alpha < \beta \leq \beta_{tu} \\ 0 & \beta > \beta_{tu} \end{cases} \quad (1)$$

$$\frac{\sigma_c(\lambda)}{E \varepsilon_{cr}} = \begin{cases} \gamma \lambda & 0 < \lambda \leq \omega \\ \gamma \omega & \omega < \lambda \leq \lambda_{cu} \\ 0 & \lambda > \lambda_{cu} \end{cases} \quad (2)$$

$$\frac{\sigma_s(\psi)}{E \varepsilon_{cr}} = \begin{cases} \gamma_s \psi & 0 < \psi \leq \zeta \\ \gamma_s \zeta & \zeta < \psi \leq \psi_{su} \\ 0 & \psi > \psi_{su} \end{cases} \quad (3)$$

where, σ_t and σ_s are the tensile stress of FRC and steel bars, respectively, and σ_c is the compressive stress of FRC. The other dimensionless parameters are obtained from the following equations (Fig. 1):

$$\alpha = \frac{\varepsilon_{trn}}{\varepsilon_{cr}}; \beta_{tu} = \frac{\varepsilon_{tu}}{\varepsilon_{cr}}; \eta = \frac{E_{cr}}{E}; \mu = \frac{\sigma_{cst}}{E \varepsilon_{cr}}; \gamma = \frac{E_c}{E}; \lambda_{cu} = \frac{\varepsilon_{cu}}{\varepsilon_{cr}} \quad (4)$$

$$\omega = \frac{\varepsilon_{cy}}{\varepsilon_{cr}}; \zeta = \frac{\varepsilon_{sy}}{\varepsilon_{cr}}; \gamma_s = \frac{E_s}{E}; \psi_{su} = \frac{\varepsilon_{su}}{\varepsilon_{cr}} \quad (5)$$

The normalized concrete tensile strain at the bottom fibre (β), normalized concrete compressive strain at the top fibre (λ), and normalized steel tensile strain (ψ) are defined as:

$$\beta = \frac{\varepsilon_{tbot}}{\varepsilon_{cr}}; \lambda = \frac{\varepsilon_{ctop}}{\varepsilon_{cr}}; \psi = \frac{\varepsilon_s}{\varepsilon_{cr}} \quad (6)$$

A linear variation of strain is assumed on the depth of the section and, hence, parameters β , λ , and ψ are linearly related together:

$$\lambda = \frac{k}{1-k} \beta; \psi = \frac{1-k-\Delta}{1-k} \beta \quad (7)$$

where k and Δ are the neutral axis depth ratio and normalized cover thickness of steel bars, respectively (Fig. 2). Regarding the material properties, nine possible strain configurations can be distinguished according to Tab. 1.

Tab. 1 Possible strain variation of the material parameters [10].

Strain configuration	FRC		Steel bars
	Tension	Compression	
1	$0 \leq \beta \leq 1$	$0 \leq \lambda \leq \omega$	$0 \leq \psi \leq \zeta$
2.1.1	$1 < \beta \leq \alpha$	$0 \leq \lambda \leq \omega$	$0 \leq \psi \leq \zeta$
2.1.2	$1 < \beta \leq \alpha$	$0 \leq \lambda \leq \omega$	$\zeta < \psi \leq \psi_{su}$
2.2.1	$1 < \beta \leq \alpha$	$\omega < \lambda \leq \lambda_{cu}$	$0 \leq \psi \leq \zeta$
2.2.2	$1 < \beta \leq \alpha$	$\omega < \lambda \leq \lambda_{cu}$	$\zeta < \psi \leq \psi_{su}$
3.1.1	$\beta > \alpha$	$0 \leq \lambda \leq \omega$	$0 \leq \psi \leq \zeta$
3.1.2	$\beta > \alpha$	$0 \leq \lambda \leq \omega$	$\zeta < \psi \leq \psi_{su}$
3.2.1	$\beta > \alpha$	$\omega < \lambda \leq \lambda_{cu}$	$0 \leq \psi \leq \zeta$
3.2.2	$\beta > \alpha$	$\omega < \lambda \leq \lambda_{cu}$	$\zeta < \psi \leq \psi_{su}$

For each value of applied normalized concrete tensile strain, β , the net force is obtained as a difference between the tensile and compression forces equated to zero for internal equilibrium, and solved for the neutral axis depth ratio k , which is obtained from the equations included in Tab. 2 for the distinct possible stages. Depending on the stage of loading (i), the resisting bending moment and the corresponding curvature (M_i, ϕ_i) of the cross section can be calculated from the following equations:

$$M_i = M'_i - M_{cr}; \phi_i = \phi'_i - \phi_{cr} \quad (8)$$

where, M'_i and ϕ'_i are the normalized moment and curvature at stage i obtained from the equations indicated in Tab. 3, while M_{cr} and ϕ_{cr} are the cracking moment and the corresponding curvature calculated for a rectangular section from the following equations:

$$M_{cr} = \frac{1}{6} b d^2 (E \varepsilon_{cr}); \phi_{cr} = \frac{2 \varepsilon_{cr}}{d} \quad (9)$$

After having been supplied the geometric characteristics and reinforcement arrangement of the cross section, as well as the parameters defining the constitutive laws of the intervening materials, an incremental procedure of the normalized concrete tensile strain at bottom fibre $\Delta\beta$ is given up to a maximum supplied limit of β (β_{max}). For the applied value of β , parameter k is obtained by trial and error using gradually the equations of Tab. 2 for stage 1 up to stage 3.2.2. The resultant force is obtained as the difference between the tensile and compression forces indicated elsewhere [10].

Tab. 2 Equation for the neutral axis depth ratio for each strain configuration [10].

Strain configuration	k
1	$k_1 = \begin{cases} \frac{2\gamma_s \rho (1-\Delta) + 1}{2\sqrt{D_1}} & \text{for } \gamma = 1 \\ \frac{-(1+\rho\gamma_s) + \sqrt{D_1}}{(\gamma-1)} & \text{for } \gamma < 1 \text{ or } \gamma > 1 \end{cases}$ $D_1 = 2\gamma_s \rho (0.5\rho\gamma_s + \gamma - \gamma\Delta + \Delta) + \gamma$
2.1.1	$k_{211} = \frac{D_{211} + \gamma_s \beta^2 \rho - \sqrt{[(D_{211} + \gamma_s \beta^2 \rho)^2 - (D_{211} - \beta^2 \gamma)(D_{211} + 2\gamma_s \beta^2 \rho - 2\gamma_s \beta^2 \rho \Delta)]}}{D_{211} - \beta^2 \gamma}$ $D_{211} = \eta(\beta^2 - 2\beta + 1) + 2\beta - 1$
2.1.2	$k_{212} = \frac{D_{212} + \zeta\gamma_s \beta \rho - \sqrt{[(D_{212} + \zeta\gamma_s \beta \rho)^2 - (D_{212} - \beta^2 \gamma)(D_{212} + \zeta\gamma_s \beta \rho)]}}{D_{212} - \beta^2 \gamma}$ $D_{212} = \eta(\beta^2 - 2\beta + 1) + 2\beta - 1$
2.2.1	$k_{221} = \frac{D_{221} + \omega\gamma\beta + \gamma_s \beta^2 \rho - \sqrt{[(D_{221} + \omega\gamma\beta + \gamma_s \beta^2 \rho)^2 - (D_{221} + 2\Delta\gamma\beta)(D_{221} + 2\gamma_s \beta^2 \rho - 2\gamma_s \beta^2 \rho \Delta)]}}{D_{221} + 2\omega\gamma\beta}$ $D_{221} = \eta(\beta^2 - 2\beta + 1) + 2\beta - 1 + \omega^2 \gamma$
2.2.2	$k_{222} = \frac{D_{222} + 2\beta\zeta\gamma_s \rho}{D_{222} + 2\omega\gamma\beta}$ $D_{222} = \eta(\beta^2 - 2\beta + 1) + 2\beta - 1 + \omega^2 \gamma$
3.1.1	$k_{311} = \frac{D_{311} + \gamma_s \beta^2 \rho - \sqrt{[(D_{311} + \gamma_s \beta^2 \rho)^2 - (D_{311} - \beta^2 \gamma)(D_{311} + 2\gamma_s \beta^2 \rho - 2\gamma_s \beta^2 \rho \Delta)]}}{D_{311} - \beta^2 \gamma}$ $D_{311} = \eta(\alpha^2 - 2\alpha + 1) + 2\alpha - 1 + 2\mu\beta - 2\mu\alpha$
3.1.2	$k_{312} = \frac{D_{312} + \zeta\gamma_s \beta \rho - \sqrt{[(D_{312} + \zeta\gamma_s \beta \rho)^2 - (D_{312} - \beta^2 \gamma)(D_{312} + 2\zeta\gamma_s \beta \rho)]}}{D_{312} - \beta^2 \gamma}$ $D_{312} = \eta(\alpha^2 - 2\alpha + 1) + 2\alpha - 1 + 2\mu\beta - 2\mu\alpha$
3.2.1	$k_{321} = \frac{D_{321} + \omega\gamma\beta + \gamma_s \beta^2 \rho - \sqrt{[(D_{321} + \omega\gamma\beta + \gamma_s \beta^2 \rho)^2 - (D_{321} + 2\Delta\gamma\beta)(D_{321} + 2\gamma_s \beta^2 \rho - 2\gamma_s \beta^2 \rho \Delta)]}}{D_{321} + 2\omega\gamma\beta}$ $D_{321} = \eta(\alpha^2 - 2\alpha + 1) + 2\alpha - 1 + \omega^2 \gamma + 2\mu\beta - 2\mu\alpha$
3.2.2	$k_{322} = \frac{D_{322} + 2\beta\zeta\gamma_s \rho}{D_{322} + 2\omega\gamma\beta}$ $D_{322} = \eta(\alpha^2 - 2\alpha + 1) + 2\alpha - 1 + \omega^2 \gamma + 2\mu\beta - 2\mu\alpha$

Tab. 3 Equation for the normalized moment and curvature for each strain configuration [10]

Strain configuration	M'
1	$M'_1 = \frac{2\beta \left[(\gamma - 1)k_1^3 + (3\gamma_s \rho + 3)k_1^2 + (6\gamma_s \rho (\Delta - 1) - 3)k_1 + 3\gamma_s \rho (\Delta - 1)^2 + 1 \right]}{(1 - k_1)}$
2.1.1	$M'_{211} = \frac{(2\beta\gamma + C_{211})k_{211}^3 + (6\gamma_s \beta \rho - 3C_{211})k_{211}^2 + (3C_{211} + 12\gamma_s \beta \rho (\Delta - 1))k_{211} + 6\gamma_s \beta \rho (\Delta - 1)^2 - C_{211}}{(1 - k_{211})}$
2.1.2	$C_{211} = \frac{-2\eta\beta^3 + 3\eta\beta^2 - 3\beta^2 - \eta + 1}{\beta^2}$
2.2.1	$M'_{212} = \frac{(2\beta\gamma + C_{212})k_{212}^3 + 3(2\gamma_s \zeta \rho - C_{212})k_{212}^2 + 3(C_{212} + 2\gamma_s \zeta \rho (\Delta - 2))k_{212} + 6\gamma_s \zeta \rho (1 - \Delta) - C_{212}}{(1 - k_{212})}$
2.2.2	$C_{212} = \frac{-2\eta\beta^3 + 3\eta\beta^2 - 3\beta^2 - \eta + 1}{\beta^2}$
3.1.1	$M'_{311} = \frac{-(3\omega\gamma + C_{221})k_{221}^3 + 3(\omega\gamma + C_{221} + 2\gamma_s \beta \rho)k_{221}^2 + 3(4\gamma_s \beta \rho (\Delta - 1) - C_{221})k_{221} + 6\gamma_s \beta \rho (\Delta - 1)^2 + C_{221}}{(1 - k_{221})}$
3.1.2	$C_{221} = \frac{2\eta\beta^3 - 3\eta\beta^2 + 3\beta^2 - \omega^3\gamma + \eta - 1}{\beta^2}$
3.2.1	$M'_{222} = (3\omega\gamma + C_{222})k_{222}^2 - 2(3\zeta\gamma_s \rho + C_{222})k_{222} + 6(\zeta\gamma_s \rho - \zeta\gamma_s \rho \Delta) + C_{222}$
3.2.2	$C_{222} = \frac{2\eta\beta^3 - 3\eta\beta^2 + 3\beta^2 - \omega^3\gamma + \eta - 1}{\beta^2}$
3.3.1	$M'_{311} = \frac{(C_{311} - 2\beta\gamma)k_{311}^3 - 3(2\gamma_s \beta \rho + C_{311})k_{311}^2 + 3(C_{311} - 4\gamma_s \beta \rho (\Delta - 1))k_{311} - 6\gamma_s \beta \rho (\Delta - 1)^2 - C_{311}}{(k_{311} - 1)}$
3.3.2	$C_{311} = \frac{3(\mu\beta^2 - \mu\alpha^2 - \eta\alpha^2 + \alpha^2) + 2\eta\alpha^3 + \eta - 1}{\beta^2}$
3.4.1	$M'_{312} = \frac{(C_{312} - 2\beta\gamma)k_{312}^3 - 3(2\gamma_s \zeta \rho + C_{312})k_{312}^2 + 3(C_{312} + 2\gamma_s \zeta \rho (2 - \Delta))k_{312} + 6\gamma_s \zeta \rho (\Delta - 1) - C_{312}}{(k_{312} - 1)}$
3.4.2	$C_{312} = \frac{3(\mu\beta^2 - \mu\alpha^2 - \eta\alpha^2 + \alpha^2) + 2\eta\alpha^3 + \eta - 1}{\beta^2}$
3.5.1	$M'_{321} = \frac{-(3\omega\gamma + C_{321})k_{321}^3 + 3(\omega\gamma + C_{321} + 2\gamma_s \beta \rho)k_{321}^2 + 3(4\gamma_s \beta \rho (\Delta - 1) - C_{321})k_{321} + 6\gamma_s \beta \rho (\Delta - 1)^2 + C_{321}}{(1 - k_{321})}$
3.5.2	$C_{321} = \frac{3(\mu\beta^2 - \mu\alpha^2 - \eta\alpha^2 + \alpha^2) + 2\eta\alpha^3 - \omega^3\gamma + \eta - 1}{\beta^2}$
3.6.1	$M'_{322} = (3\omega\gamma + C_{322})k_{322}^2 - 2(3\zeta\gamma_s \rho + C_{322})k_{322} + 6(\zeta\gamma_s \rho - \zeta\gamma_s \rho \Delta) + C_{322}$
3.6.2	$C_{322} = \frac{3(\mu\beta^2 - \mu\alpha^2 - \eta\alpha^2 + \alpha^2) + 2\eta\alpha^3 - \omega^3\gamma + \eta - 1}{\beta^2}$

$$f_i^{\sim} = \frac{b}{2(1 - k_i)}$$

If the resultant force is smaller than a given force tolerance value, the correct value of k is obtained, otherwise the trial procedure continues in the following stage. After having been obtained the correct value of the k parameter and the stage number, the normalized moment (M'_i) and the corresponding curvature (ϕ'_i) are calculated from the equations included in Tab. 3. These values are introduced in Eq. 8 to calculate the moment and curvature due to that specific normalized tensile strain. This incremental-iterative process is terminated when the normalized concrete tensile strain at bottom fibre attains β_{max} .

Using the obtained moment-curvature relationship, the force-deflection response of a statically determinate beam failing in bending can be determined. The beam is discretized in Euler-Bernoulli beam elements of 2 nodes. The tangential or the secant flexural stiffness of each element, $(EI)_{Te}$, is determined from its moment-curvature relationship that is stored in a data file (each element has its own $M-\phi$ file). Therefore, the present approach can simulate the deformability of a beam composed of zones of distinct moment-curvature, giving to the model the possibility of predicting with enough accuracy the force-deflection response of quite heterogeneous beams in terms of material constitutive laws and arrangements of the materials, if these constitutive laws are known [11]

4. Model appraisal

To evaluate the predictive performance of the proposed model, an experimental program with shallow beams of steel fibre reinforced self-compacting concrete (SFRSCC) was carried out. The mix composition adopted for the manufacture of the SFRSCC was optimized for a solid skeleton that includes 45 kg/m³ of hooked end steel fibres (SF) of a length (l_f) of 60 mm, a diameter (d_f) of 0.75 mm, an aspect ratio (l_f/d_f) of 80 and a yield stress of 1100 MPa. The performed experimental program included three series of shallow beams, submitted to a four points load configuration (Fig. 3).

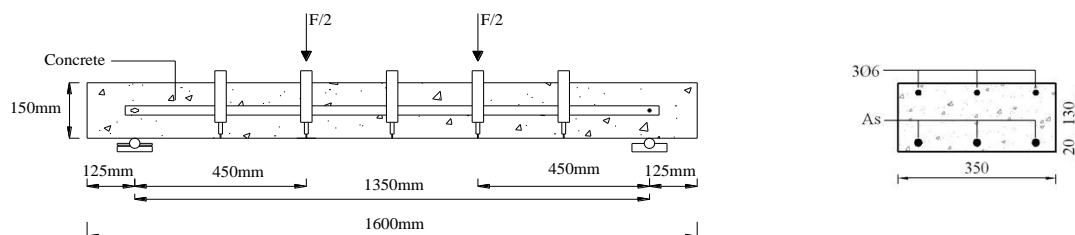


Fig. 3: Dimensions (in mm), support and load conditions, and monitoring system.

Using 3 ϕ 6, 3 ϕ 8 and 3 ϕ 10 of steel bars for the series of beams designated by A-6-45, B-8-45 and C-10-45, respectively, the influence of the reinforcement ratio on the effectiveness of the fibre reinforcement can be assessed. In all beams three steel bars of 6 mm diameter were used in the top part of the cross section, which contribution was, however, disregarded in the numerical simulations. The force was applied by a load cell of 300 kN capacity, and the deflections were measured by five LVDT's. The values of the parameters of the constitutive model are indicated in Tab. 4.

Tab. 4 - Values computed for the constitutive models for series of beams

Series' designation	E (GPa)	ε_{cr} (%)	α	μ	β_{tu}	γ	ω	λ_{cu}	ρ (%)	γ_s	ζ	ψ_{su}
A-6-45	45	0.01	2.5	0.6	30	1.0	25.96	37.5	0.2	4.51	28	100
B-8-45	45	0.01	2.5	0.6	43	1.0	25.96	37.5	0.36	4.33	30	143
C-10-45	45	0.01	2.5	0.6	43	1.0	25.96	37.5	0.56	4.38	30	115

The force-deflection curves predicted by the numerical approach and recorded in the experimental tests are compared in Fig. 4, from which it can be concluded that the predictive performance of this approach is quite good for design purposes of FRC elements failing in bending.

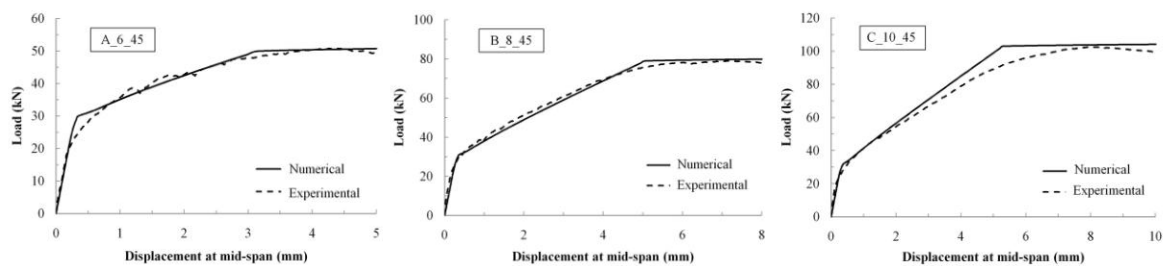


Fig. 4: Evaluation of the predictive performance of the developed model.

5. Conclusions

In the present work, a closed form solution was developed to predict the moment-curvature relationship of rectangular cross sections of strain-hardening or strain-softening fibre reinforced concrete (FRC) beams that can also include tensile longitudinal steel bars. The moment-curvature relationship was used as the entity capable of supplying the tangential or the secant flexural stiffness of small elements that discretize a statically determinate beam, in order to predict its force-deflection response. The predictive performance of this design-oriented approach was evaluated in an experimental program composed of three series of shallow steel fibre reinforced self-compacting concrete beams with distinct percentage of longitudinal steel bars. The predictive performance evidences that the developed strategy can be adopted by designers, since the obtained levels of accuracy are quite satisfactory, taking into account the adopted simplifications, in order to turn the model of simple implementation.

Acknowledgements

This work is part of the research project QREN number 3456, PONTALUMIS-Development of a prototype of a pedestrian bridge in GFRP-ECC concept, involving the Company ALTO - Perfis Pultrudidos, Lda., the ISISE/ University of Minho and the ICIST/Technical University of Lisbon. The first and third authors wish to acknowledge the research grants under this project. The authors also wish to acknowledge the Civitest Company for the conception and development of the steel fiber reinforced self-compacting concrete used in this work.

6. Reference

- [1] J.A.O. Barros, “Steel fiber reinforced self-compacting concrete – from the material characterization to the structural analysis”, *HAC2008, 1st Spanish Congress on Self-Compacting Concrete, Valencia, Spain*, 31-58, 18-19 February, 2008. (Invited Keynote Lecturer)
- [2] V.M.C.F. Cunha, J.A.O. Barros, J.M. Sena-Cruz, “Pullout behaviour of steel fibres in self-compacting concrete”, *ASCE Journal of Materials in Civil Engineering*, 22(1), January 2010.
- [3] C. Soranakom, B. Mobasher, “Correlation of tensile and flexural response of strain softening and strain hardening cement composites”, *Cement & Concrete Composites*, 30, 465-477, 2008.
- [4] A. E. Naaman, H. W. Reinhard, “Proposed classification of HPFRC composites based on their tensile response”. In N. Banthia, A. B., T. Uomoto & Shah, S., eds., *Proceedings 3rd international Conference on Construction materials: Performance, Innovations and Structural Implications (ConMat'05) and Mindess Symposium*, p. 458. University of British Columbia, Vancouver, Canada, Vancouver, Canada, 2005.
- [5] C. Soranakom, “Multi scale modeling of fibre and fabric reinforced cement based composites”, *PhD thesis*, Arizona State University, 2008.
- [6] H. Salehian, J. A.O. Barros, M. Taheri, “A design-based approach to estimate the moment curvature relationship of element made from fibre reinforced concrete and strengthened by longitudinal steel bars– implementation and parametric studies”, *Technical report A0.T0.UM.1, PONTALUMIS project*, Dep. Civil Eng., School of Eng., University of Minho, Guimaraes, Portugal, 2010.
- [7] V.M.C.F. Cunha, J.A.O. Barros, J.M. Sena-Cruz, “Tensile behavior of steel fiber reinforced self-compacting concrete”, Session “Fiber-Reinforced Self-Consolidating Concrete”, Salons G&H, Hotel Marriott, New Orleans USA, 11 November de 2009.
- [8] A. P. Fantilli, H. Mihashi, P. Vallini, “Multiple cracking and strain hardening in fibre-reinforced concrete under uniaxial tension”, *Cement and Concrete Research* 39, 1217-1229, 2009.
- [9] V.M.C.F. Cunha, J.A.O. Barros, J.M. Sena-Cruz, “Modelling the influence of age of steel fibre reinforced self – compacting concrete on its compressive behaviour”, *RILEM Materials and Structures Journal*, 41(3), 465-478, 2008.
- [10] M. Taheri, J.A.O. Barros, H. Salehian, “A design model for strain-softening and strain-hardening fiber reinforced elements reinforced by longitudinal steel bars failing in bending – implementation and parametric studies”, Technical report 06-DEC/E-10, Dep. Civil Eng., School Eng. University of Minho, March 2010.
- [11] J.A.O. Barros, J.T. Oliveira, P.J.B. Lourenço, E. Bonaldo, “Flexural behavior of reinforced masonry panels”, *ACI Structural Journal*, 13(3), May-June, 418-426, 2006.